Biogeosciences Discuss., 5, 4919–4944, 2008
www.biogeosciences-discuss.net/5/4919/2008/

Biogeosciences Discussions

Biogeosciences Discussions is the access reviewed discussion forum of *Biogeosciences*

Modelling the vertical distribution of bromoform in the upper water column of the tropical Atlantic Ocean

I. Hense[1] **and B. Quack**[2]

[1]Leibniz Institute for Baltic Sea Research, Rostock, Germany
[2]Leibniz Institute of Marine Sciences, IFM-GEOMAR, Kiel, Germany

Received: 30 September 2008 – Accepted: 17 October 2008 – Published: 16 December 2008

Correspondence to: I. Hense (inga.hense@io-warnemuende.de)

Published by Copernicus Publications on behalf of the European Geosciences Union.

Abstract

The relative importance of potential source and sink terms for bromoform ($CHBr_3$) in the tropical Atlantic Ocean is investigated with a coupled physical-biogeochemical water column model. Bromoform production is either assumed to be linked to primary production or to phytoplankton losses; bromoform decay is treated as light dependent (photolysis), and in addition either vertically uniform, proportional to remineralisation or to nitrification. All experiments lead to the observed subsurface maximum of bromoform, corresponding to the subsurface phytoplankton biomass maximum. In the surface mixed layer, the concentration is set by entrainment from below, photolysis in the upper few meters and the outgassing to the atmosphere. The assumed bromoform production mechanism has only minor effects on the solution, but the various loss terms lead to significantly different bromoform concentrations below 200 m depth. The best agreement with observations is obtained when the bromoform decay is coupled to nitrification (parameterised by an inverse proportionality to the light field). Our model results reveal a pronounced seasonal cycle of bromoform outgassing, with a minimum in summer and a maximum in early winter, when the deepening surface mixed layer reaches down into the bromoform production layer.

1 Introduction

A considerable part of the ozone destruction in the troposphere and stratosphere is attributed to bromine species (see, e.g. Prather et al., 1984; Platt and Hönninger, 2003; von Glasow et al., 2004; Sinnhuber and Folkins, 2006) formed from bromoform ($CHBr_3$) of oceanic origin. Hence, bromomform sources and sinks in the ocean are of interest for studying atmospheric trace gas cycles. Particularly high atmospheric concentrations of bromine species (see Read et al., 2008) and corresponding air-sea fluxes of $CHBr_3$ (Quack et al., 2004) have been found in the tropics and subtropics, both offshore and in coastal regions.

BGD

5, 4919–4944, 2008

Recent $CHBr_3$ observations in the tropical eastern Atlantic Ocean (Quack et al., 2004, 2007) have revealed a pronounced subsurface maximum in the depth of the subsurface chlorophyll maximum, suggesting a phytoplanktonic source of bromoform. This is consistent with laboratory experiments and field data that suggest a coupling between bromoform production and phytoplankton growth for diatoms and cyanobacteria (Moore et al., 1996; Schall et al., 1996; Karlsson et al., 2008). Whether $CHBr_3$ production serves a specific purpose (e.g., protection against grazing and cell poisoning by hydrogen peroxide – see e.g. Manley, 2002) or has to be regarded as the byproduct of another process is currently not known. It can also not be ruled out that bromoform is produced during the decay of organic matter, i.e. phytoplankton (Quack and Wallace, 2003) when the enzyme bromoperoxidase (necessary to catalyse the reaction with bromide ions) is set free. Whichever it may turn out to be, a close link to growth and/or decay of phytoplankton seems highly plausible. Alternative ideas about open ocean bromoform sources (coastal production by macroalgae and/or advective transport, see e.g., Moore and Tokarczyk, 1993; Carpenter and Liss, 2000) are not considered here for this region.

Several processes have been found responsible for the reduction of $CHBr_3$ concentrations in the ocean: Outgassing to the atmosphere may be the major factor in the surface mixed layer (see Quack et al., 2004). Other known decay processes include halide substitution of $CHBr_3$ which leads to an estimated oceanic half life between 5 and 74 years (at 25°C and 2°C, respectively) as well as hydrolysis working ten to hundred times slower (Geen, 1992; Vogel et al., 1987). In addition, it is assumed that photolysis plays an important role in the decay of $CHBr_3$ in the surface ocean (Carpenter and Liss, 2000). Several biologically mediated processes including the decomposition of organic material by bacteria (Fetzner, 1998) accelerate bromoform degradation. Recent observations indicate also a co-metabolism of bromoform during nitrification: The decay of bromoform has been shown to be more rapid in the presence of *Nitrosomonas* which oxidizes ammonium to nitrite (Wahman et al., 2005). The pronounced nitrite maximum below the subsurface chlorophyll maximum layer in the oligotrophic

BGD
5, 4919–4944, 2008

open ocean (data from Meteor expedition M55, Wallace and Bange, 2004) might be an indication of not only nitrification[1], i.e. ammonium oxidation (Olson, 1981), but also enhanced bromoform decomposition. Observational evidence of a decrease of $CHBr_3$ in the nitracline, where nitrification is usually maximum, exists (Quack, unpublished data from the Meteor cruise 60/5).

In summary, the magnitude of water column losses, their vertical distribution and their effect on surface mixed layer bromoform concentrations and the associated outgassing are only poorly known (see e.g., Abrahamsson et al., 2004). In this study, we use numerical modelling to elucidate the role of different sources and sinks of open ocean $CHBr_3$ in controlling the oceanic bromoform levels and the resulting air-sea flux.

2 Model setup

2.1 Physical model setup

The physical model is the one-dimensional water column model GOTM (General Ocean Turbulence Model, Umlauf et al., 2005, www.gotm.net). The model has been previously applied to several oceanic regimes, including the subtropical oligotrophic North Atlantic Ocean (BATS: Bermuda Atlantic Time-series Study, Weber et al., 2007) and the Baltic Sea (Burchard et al. 2006).

Here, GOTM is configured for the eastern tropical North Atlantic Ocean for the Cape Verde region. The model set-up is based on the BATS case, with only few modifications: a relatively high minimum value for turbulent kinetic energy (TKE) of $10^{-5}\,m^2\,s^{-2}$ is prescribed to parameterise the effects of double diffusion in this region (see e.g., Martínez-Marrero et al., 2008). In addition, we have applied the bulk air-sea parameterisation for heat and freshwater fluxes of Fairall et al. (1996). The model covers the upper 700 m of the ocean; the lower boundary has been placed at this depth because it

[1]One has to keep in mind, however, that uncertainties exist concerning the mechanisms leading to the nitrite signal (see, e.g. Lomas and Lipschultz, 2006).

is close to the nutrient maximum where the diffusive fluxes vanish (see also Beckmann and Hense, 2007). The vertical resolution is 1 m and the time step 1 h.

2.2 Biogeochemical model setup

Our ecosystem model is based on the relatively simple nitrogen-phytoplankton-zooplankton-detritus (*NPZD*) model of Schartau and Oschlies (2003). Weber et al. (2007) have coupled it to GOTM for their study of the oligotrophic situation at BATS; we found no need to change any of their model parameters. For our purposes, we have added a bromoform compartment B (in nmol $CHBr_3$ m^{-3}) that evolves due to internal sources (Q) and sinks (S) as well as vertical diffusion:

$$\frac{\partial B}{\partial t} = Q - S + \frac{\partial}{\partial z}\left(A_v \frac{\partial B}{\partial z}\right)$$

where A_v is the time- and depth-dependent turbulent vertical diffusivity coefficient.

The source terms are either coupled to primary production (Q_1) or to the total phytoplankton losses (Q_2)

$$Q_1 = \beta \cdot \mu \cdot P$$

$$Q_2 = \beta^* \cdot (\gamma \cdot P^2 + r \cdot P + g_Z \cdot Z)$$

Here, P and Z are the phytoplankton and zooplankton concentrations, respectively (in mmol N m^{-3}), μ is the actual (in situ) growth rate of phytoplankton, γ is the mortality rate of phytoplankton, r and g_Z are phytoplankton respiration and phytoplankton-dependent grazing rates of the *NPZD* model. We call the bromoform production to phytoplankton production ratio β, and a conceptually similar bromoform production to phytoplankton loss ratio β^*.

These proportionality factors were computed based on a suite of laboratory studies which report bromoform increase during the exponential growth phase of phytoplankton (Moore et al., 1996). First, we extracted the maximum specific growth rates ω

BGD
5, 4919–4944, 2008

of the three species under investigation from the exponential phase[2]; then the corresponding temporal changes in bromoform concentrations ($\Delta CHBr_3$) over time interval Δt were used to determine the bromoform production to phytoplankton production ratio according to

$$\beta = \frac{\Delta CHBr_3}{\Delta t \cdot \omega P_0} \cdot e^{-\omega \Delta t}$$

The resulting values for β are 4.2, 6.71, and 6.73×10^{-7} nmol $CHBr_3$ $(\text{mmol N})^{-1}$, using typical cellular carbon contents of the species (Wasmund, pers comm.: 176 pg C cell^{-1} for *Nitzschia sp.* and *Nitzschia arctica*, 2015 pg C cell^{-1} for *Porosira glacialis*) and the Redfield ratio for conversion into nitrogen. The first value stems from an experiment (with *Nitzschia arctica*) which has been terminated prematurely (i.e., during the exponential growth phase). We therefore choose the average of the other two $\beta = 6.72 \times 10^{-7}$ nmol $CHBr_3$ $(\text{mmol N})^{-1}$ for our numerical experiments, assuming that this value (obtained for cold water diatoms) is generally appropriate for other species and phytoplankton groups. Not only do we assume that many more species do produce bromoform, but also that the rate is relatively constant across the phytoplankton assemblage. Supporting evidence for the first assumption is that bromoperoxidase enzymes which are necessary for bromoform production have been identified for diatoms, cyanobacteria, and Prymnesiophyceae (Moore et al., 1996; Jakopitsch, 2001; Hughes et al., 2006; Karlsson et al., 2008). We realise that the second assumption may be more problematic, but to our knowledge there are no studies that disprove it. This is an area that needs further research.

An alternative interpretation of the laboratory experiments by Moore et al. (1996) is that bromoform production is correlated with the release of bromoperoxidase from the phytoplankton cell as a result of respiration and during the death of the cell. Hence,

[2]Since temporal changes (Δt) in cell counts are the result of the actual growth rate but not the maximum specific growth rate, we account for a respiration of 1% d^{-1}.

a similar approach leads to the formulation Q_2 and β^* can be determined from the decay phase in Moore et al. (1996)'s experiments. These data are more difficult to extract, but it seems that β^* is close to β, so for simplicity we assume them to be equal.

Bromoform is lost from the ocean through outgassing:

$$F|_{z=0} = k \cdot \left(B_{\text{equi}} - B|_{z=0}\right)$$

using the gas transfer velocity k after Nightingale et al. (2000) and the atmospheric equivalent concentration B_{equi} (based on the parameterisation by Moore et al., 1995).

Four different processes are assumed to play a role as internal sinks for bromoform: photolysis, halide substitution and hydrolysis, degradation during remineralisation of detritus and nitrification.

Photolysis is considered in all experiments. We use a depth-decreasing time scale for degradation by ultraviolet radiation according to

$$S_0 = l_{uv} \cdot \frac{\mathrm{I}_0}{\mathrm{I}_{\text{ref}}} \cdot \exp(-a_w \cdot z) \cdot B$$

where I_0 denotes the instantaneous surface irradiance, I_{ref} is the annual average irradiance for the uppermost meter in this region ($75\,\mathrm{W\,m^{-2}}$), a_w the attenuation coefficient for UV-light ($0.33\,\mathrm{m^{-1}}$) and z the depth (positive downward). The decay time scale $(l_{uv})^{-1}$ is 30 days as given by Carpenter and Liss (2000). Due to the short penetration depth of ultraviolet radiation, photolysis can only play a role in the surface mixed layer. In addition, we have implemented the following loss terms:

– halide substitution and hydrolysis is assumed to be constant throughout the water column. A constant decay rate l_{con} for $CHBr_3$ is used, where the exponential time scale $(l_{\text{con}})^{-1}$=6.33 years (a half life of 4.37 years) is at the lower end of the range of the estimated half life of bromoform (halide substitution, hydrolysis) from observations (5–74 years, Quack and Wallace, 2003):

$$S_1 = S_0 + l_{\text{con}} \cdot B$$

This approach is the most simple choice, as it requires the specification of only one parameter.

– bromoform degradation related to the remineralisation of detritus (D) (following Fetzner, 1998) using an exponential decay time scale of $(l_{\text{rem}})^{-1}$=7.92 years (half life: 5.49 years), and taking into account the temperature dependence for remineralisation from the *NPZD* model:

$$S_2 = S_0 + l_{\text{rem}} \cdot \frac{D}{D_{\text{ref}}} \cdot 1.066^T \cdot B$$

The reference concentration for detritus is D_{ref}=0.13 mmol N m^{-3}.

– as a (crude) parameterisation for the degradation of $CHBr_3$ by nitrifiers the decay rate has been inversely coupled to the light field I, assuming that nitrification (ammonium oxidation) is inhibited by high light levels (Olson, 1981). To our knowledge, no empirical information exists about the light dependence of nitrification limitation. We therefore adopt the functional dependence of the phytoplankton light limitation to describe this process based on 24 h averages of irradiance:

$$S_3 = S_0 + l_{\text{nit}} \left(1 - \frac{\frac{a}{24\,\text{h}} \int_{t-24\,\text{h}}^{t} \text{I}(z) dt}{\sqrt{\lambda^2 + \left(\frac{a}{24\,\text{h}} \int_{t-24\,\text{h}}^{t} \text{I}(z) dt \right)^2}} \right) \cdot B$$

The exponential decay time scale is assumed to be $(l_{\text{nit}})^{-1}$=4 years (half life: 2.74 years); the additional parameters are a=3.0×10^{-5} m^2 W^{-1} s^{-1} and λ=3.1×10^{-6} s^{-1}.

In this paper, we shall present results from four experiments, which use different combinations of source and sink terms (see Table 1).

BGD
5, 4919–4944, 2008

2.3 Forcing and initialisation

The model is forced by climatological monthly means of 2-m atmospheric temperature, air pressure and dew point temperature, 10-m zonal and meridional wind velocities, cloud cover as well as precipitation based on ERA40 reanalysis (Uppala et al., 2005). The physical variables temperature and salinity are initialised with climatological profiles from the World Ocean Atlas (WOA01) (Conkright et al., 2002). Lateral effects in the one-dimensional model are taken into account by restoring salinity and temperature (except for the upper 20 m) towards climatological monthly means of WOCE with a five day-timescale. All biogeochemical variables are initialised homogeneously except nitrogen for which the vertical profile of dissolved inorganic nitrogen derived from measurements at Cape Verde (Bange, 2007) has been taken. At the bottom, the DIN concentration is restored to the observed value of 35.7 mmol m^{-3} with a relaxation time scale of one hour. The atmospheric concentration of $CHBr_3$ is set constant, using a value of 0.14 nmol m^{-3} (3.4 ppt) which is a mean (and typical) value for atmospheric bromoform concentrations in that particular region (Quack et al., 2004). Although initialization and forcing fields are from Cape Verde at 17.4° N, 24.5° W, we believe that our results are representative for the entire eastern tropical Atlantic Ocean.

3 Results and discussion

The model has been run for 50 years after which a perpetual seasonal cycle has developed; we have analysed the last year. The relatively long spin-up time is required for the slowly evolving bromoform distributions. The physical fields reach a periodically steady state after about 6 years, the biological variables after about 10 years.

BGD
5, 4919–4944, 2008

3.1 Hydrographic and biogeochemical characteristics

Our simulation of the physical conditions at Cape Verde reproduce the temperature and salinity fields reasonably well (Fig. 1). The annual mean vertical profile of salinity shows a subsurface salinity maximum in about 100 m depth (Fig. 1a) which is a feature of the tropical eastern North Atlantic Ocean resulting from the salt water intrusion from the South Atlantic, the SACW (South Atlantic Central Water). As expected for this region, the main thermocline is found between 50 and 100 m (Fig. 1b).

The annual mean vertical profile of nutrients shows a depletion in the upper 50 m (Fig. 1) due to the uptake by phytoplankton and subsequent sinking of dead organic matter. The maximum concentrations of phytoplankton biomass are found subsurface in the upper nutricline where light and nutrient supply are optimal. This is in agreement with observations in that region (Quack et al., 2004; Bahamón et al., 2003). Due to sinking, the detritus maximum is located below the phytoplankton maximum.

3.2 Vertical distribution of bromoform

As expected for a phytoplankton related source of $CHBr_3$ in the oligotrophic ocean, the simulated annual mean vertical distribution of bromoform shows a pronounced subsurface maximum in all experiments (Fig. 2, Table 1). The maxima are located in 66 m depth, a few meters below the phytoplankton biomass maximum and occur at the depth of the strongest temperature and nutrient gradient.

We note that differences between the experiments are smallest at the surface and largest below 200 m depth. The surface concentrations are controlled by the air-sea flux, photolysis and entrainment, which are similar in all experiments (Fig. 3). The subsurface concentration of $CHBr_3$ in the water column, however, depends strongly on the assumed internal decay process (Fig. 3d).

The most striking difference between our experiments are the comparatively high concentrations of $CHBr_3$ below 200 m depth in EXP2 (Fig. 2, green line). This means that degradation coupled to remineralisation leads to high concentrations at depth, be-

BGD
5, 4919–4944, 2008

cause most of the remineralisation takes place above 200 m depth. Hence, all the bromoform that escapes into the deep ocean will accumulate there. This feature is related to the biogeochemical model and its values for detrital sinking and remineralisation rates. The few available observational data of $CHBr_3$ concentrations below 200 m show that the concentration at 630 m is close to 1.0 nmol $CHBr_3$ m^{-3} (Quack, unpublished data, 2004). While similar concentrations can be found for EXP1, EXP3 and EXP4 (0.8–1.3 nmol $CHBr_3$ m^{-3}), they are significantly higher in EXP2 (6.5 nmol $CHBr_3$ m^{-3}) indicating that the degradation is underestimated. One obvious way to decrease the deep $CHBr_3$ concentrations in EXP2 is to increase l_{rem}, but this erodes the subsurface maximum to the point of being unrealistic.

The other three experiments show similar vertical profiles. In particular, we note that the type of bromoform source (Q_1 vs. Q_2) has hardly an effect on the annual mean profiles[3]. This is both encouraging and disappointing: on the one hand we do not need to know more about the details of the production process to obtain a realistic result; on the other hand we cannot use our experiments to distinguish the different hypotheses. The highest maxima and the largest gradients of bromoform are produced in EXP3 and EXP4 (Fig. 2, red lines). A slightly reduced subsurface maximum of $CHBr_3$ and higher concentrations in 700 m depth are found in EXP1 (Fig. 2, blue curve).

A more quantitative evaluation of the model results can be performed for the month of November. Observations of bromoform in the eastern North Atlantic Ocean down to 200 m are available for a number of stations from a cruise in the beginning of November 2002 (Quack et al., 2004). Spatial (and to a lower degree temporal) variability yields profiles that differ in the depth, thickness and amplitude of bromoform maximum layers. Our one-dimensional water column model, forced by climatological fields, does not represent an individual observed profile. Therefore, we have constructed a "typical" (averaged) $CHBr_3$ distribution, applying the method of Hense and Beckmann (2008):

[3]However, we do find a time delay of about two days in the seasonal succession of bromoform production for EXP4 compared to EXP3, simply because primary prodcution precedes mortality and grazing.

Instead of averaging along depth horizons, all the maxima are aligned to obtain a "mean" profile (Fig. 4). The advantage of this approach is that two important characteristics of the distributions (amplitude and thickness) are reliably preserved while the drawback is that absolute depth information is lost (see Hense and Beckmann, 2008). Figure 4 should therefore be used only to compare amplitude and thickness between this composite of observations and the simulated profiles.

The model–data comparison for EXP1–EXP3 shows that the simulated vertical distribution patterns of $CHBr_3$ capture the most important features of the observations: the magnitude of the subsurface maximum, a strong decrease upward to the surface and a somewhat slower decrease downward (Fig. 4). Given the uncertainties of model parameters and forcing, the robustness of the results support the validity of our assumptions.

The systematic overestimation of the surface concentration in all models may be due to the use of a constant atmospheric bromoform concentration and the climatological wind fields which both affect the air-sea flux. Additional sensitivity experiments indicate that slightly changed atmospheric data can easily account for concentration changes of 2 nmol $CHBr_3$ m^{-3} in the surface mixed layer.

Differences between simulations and observations occur also with respect to the thickness of the bromoform maximum layer. The observed "typical" profile of bromoform has a thickness of about 60 m (based on a "full width at half maximum" criterion). The simulated profiles show thicker maximum layers (EXP1: 105 m, EXP2: 126 m, EXP3 and EXP4: 100 m), most likely due to an overestimation of the thickness of the subsurface biomass maximum by the ecosystem model. Simultaneous measurements of bromoform and phytoplankton biomass at high vertical resolution would be required to make conclusive statements in this respect.

As mentioned before, the largest maxima and the steepest downward gradients of bromoform are obtained for S_3, the "nitrification case" (Fig. 4, red curve). This is a consequence of the vertical separation of the production layer from the destruction layer below. It seems that the observed profiles can be best explained by adjacent, non-

overlapping internal source and sink regions.

The quantitative evaluation of our model results shows that the concentration in the subsurface maximum is best represented by EXP3 or EXP4 (Table 1). Overall, however, the differences in the concentrations of bromoform in the upper 200 m between the experiments, particularly EXP1 and EXP3 are rather small. This is also true with respect to air-sea fluxes: The simulated flux from the ocean into the atmosphere ranges only between 163–188 pmol $CHBr_3$ m^{-2} h^{-1} for November for the individual experiments. They are close to the observed 175 pmol $CHBr_3$ m^{-2} h^{-1} in this region (Table 1).

A sensitivity experiment with photolysis as the only internal loss process resulted in an imbalance between sources and sinks below the subsurface maximum and lead to unrealistically high and continuously increasing subsurface bromoform concentrations (no steady state is reached within 100 years of model integration). Vice versa, omitting photolytic destruction leads to an increase in the surface concentrations and a higher air-sea flux (8–36%).

In summary, EXP3 shows the best agreement with observations and thus, for further analyses, we focus on the results of this case.

3.3 Simulated seasonal cycle of bromoform and air-sea fluxes

Having established that the model does represent the main features of the observed bromoform distribution reasonably well, we can now look at unobserved aspects of the problem, e.g., the seasonal cycle. The highest subsurface maximum of bromoform (>24 nmol $CHBr_3$ m^{-3} at around 66 m) occurs in late autumn while the lowest concentrations can be found in spring (<18 nmol $CHBr_3$ m^{-3} in about 80 m, Fig. 5).

We note a time delay of about one month between the occurrence of the subsurface maximum and the occurrence of the surface mixed layer maximum, related to the gradual deepening of the surface mixed layer and the entrainment of the bromoform signal (Figs. 5, 6). The lowest subsurface concentrations are found in April. During spring and summer, the surface layer is essentially decoupled from the subsurface bromo-

BGD
5, 4919–4944, 2008

form production layer and the surface concentrations decrease until early August.

The seasonal cycle of bromoform surface concentration and air-sea flux shows winter maxima and summer minima (Fig. 6). Concentrations vary by a factor less than two, fluxes by a factor of almost ten. It is important to note that the seasonal flux variations are only partly caused by the variations in production; the variability in mixed layer depth, which in turn is driven by changes in heat and freshwater fluxes as well as the wind speed, is the main factor. While the absolute maximum of the air-sea flux occurs in winter, secondary maxima are found in early summer and autumn (Fig. 6). From April to June relatively high wind velocities (Fig. 6c) promote the outgassing from the surface ocean. In September and October, the combined effect of the increasing wind speed and the deepening of the mixed layer (Fig. 6a,c) inducing the entrainment of bromoform into the surface layer leads to a rapid increase in the air-sea flux (Fig. 6b). We notice that the temporal variation of bromoform in the water column is similar in all our experiments irrespective of differences in the absolute subsurface concentrations.

4 Summary and conclusions

We have simulated the climatological seasonal cycle of the vertical distribution of bromoform in the upper 700 m of the tropical eastern Atlantic Ocean. Using the results from laboratory experiments (Moore et al., 1996) bromoform production has been coupled to the growth and losses of phytoplankton, respectively. The differences between these two approaches are marginal and leave open which physiological processes are ultimately responsible for the production of $CHBr_3$. The generally good agreement of the model results with observations, however, suggests that the subsurface maximum can be entirely explained by in-situ production in which phytoplankton plays the most important role. This result is of more general relevance because observations indicate that the subsurface bromoform maximum is an ubiquitous feature of the eastern tropical Atlantic Ocean (Quack et al., 2004, 2007).

Our numerical experiments with different degradation mechanisms of $CHBr_3$ show

BGD
5, 4919–4944, 2008

that besides the near surface processes photolysis and air-sea flux, additional water column losses are necessary to explain the downward decrease in concentrations below the subsurface maximum. Among the three cases we compared, the experiment with a degradation proportional to nitrification (parameterised by an inverse proportionality to the light field) is in best agreement with observations, i.e., has the highest maximum and the lowest deep concentration of bromoform. This is achieved by the vertical separation of the bromoform production layer from the bromoform destruction layer below. In the assessment of our model results we have to keep in mind that although we have investigated the various bromoform degradation mechanisms individually, they are likely to be active simultaneously (at unknown relative strengths). In any case, nitrification-related degradation of bromoform seems essential in generating the observed vertical bromoform distribution. This is not an unreasonable result, given that observations point at a co-metabolism of $CHBr_3$ in the presence of nitrifiers (Wahman et al., 2005). In addition, recently obtained field data show a maximum of dibromomethane (a degradation product of $CHBr_3$ from reductive debromination processes) below the maximum of $CHBr_3$ (Quack, unpublished data, 2004, Butler et al., 2007). Further studies on subsurface bromoform degradation are clearly needed.

The model results further suggest that the seasonality of oceanic bromoform outgassing is larger than often assumed. While surface concentrations range from 5 to 8 nmol $CHBr_3$ m^{-3} (summer versus winter), the air-sea flux varies by almost an order of magnitude. Strongly controlled by the seasonal changes in wind speed and mixed layer depth, outgassing is 40 pmol $CHBr_3$ $m^{-2}\,h^{-1}$) in summer and 360 pmol $CHBr_3$ $m^{-2}\,h^{-1}$ in winter. Note that the use of seasonally varying atmospheric concentrations of $CHBr_3$ will lead to (probably minor) quantitative changes in these values.

The vertically integrated annual production rate of bromoform in the model is 4.6 µmol $CHBr_3$ $m^{-2}\,a^{-1}$ (525 pmol $CHBr_3$ $m^{-2}\,h^{-1}$) with a corresponding annual mean air-sea flux of 1.1–1.3 µmol $CHBr_3$ $m^{-2}\,a^{-1}$ (125–148 pmol $CHBr_3$ $m^{-2}\,h^{-1}$) for the different experiments; i.e., about 25% of the production is transferred to the atmosphere. There, as a carrier of bromine, $CHBr_3$ of phytoplanktonic origin will contribute to the

BGD
5, 4919–4944, 2008

destruction of ozone and thus should be included in budget calculations.

Acknowledgements. Valuable comments by and fruitful discussions with Aike Beckmann have substantially improved the manuscript.

This study has been financed by the German BMBF project SOPRAN 03F0462.

References

Abrahamsson, K., Lorén, A., Wulff, A., and Wangberg, S.-A.: Airsea exchange of halocarbons: the inuence of diurnal and regional variations and distribution of pigments, Deep-Sea Res. Pt. II, 29, 2789–2805, 2004. 4922

Bahamón, N., Velasquez, Z., and Cruzado, A.: Chlorophyll-a and nitrogen flux in the tropical North Atlantic Ocean, Deep-Sea Res. Pt. I, 50, 1189–1203, 2003. 4928

Bange, H. W.: Physical oceanography at CTD station PO320, Cruise report R.V. Poseidon, cruise PO320/1, IFM-GEOMAR, Leibniz-Institut für Meereswissenschaften an der Christian-Albrechts-Universität, Kiel, 2007. 4927

Beckmann, A. and Hense, I.: Beneath the surface: Characteristics of oceanic ecosystems under weak mixing conditions – a theoretical investigation, Prog. Oceanogr., 75, 771–796, 2007. 4923

Butler, J. H., King, D. B., Lobert, J. M., Montzka, S. A., Yvon-Lewis, S. A., Hall, B. D., Warwick, N. J., Mondeel, D. J., Aydin, M., and Elkins, J. W.: Oceanic distributions and emissions of short-lived halocarbons, Global Biogeochem. Cy., 21, GB1023, doi:10.1029/2006GB002732, 2007. 4933

Carpenter, L. and Liss, P. S.: On temperate sources of bromoform and other reactive organic bromine gases, J. Geophys. Res., C, 105, 20 539–20 547, 2000. 4921, 4925

Conkright, M. E., Locarnini, R. A., Garcia, H. E., O'Brien, T. D., Boyer, T. P., Stephens, C., and Antonov, J. I.: World Ocean Atlas 2001: Objective Analyses, Data Statistics, and Figures, CD-ROM Documentation, Tech. rep., National Oceanographic Data Center, Silver Spring, MD, 2002. 4927

Fairall, C. W., Bradley, E. F., Rogers, D. P., Edson, J. B., and Young, G. S.: Bulk parameterization of air-sea fluxes for tropical ocean-global atmosphere coupled-ocean atmosphere response experiment, J. Geophys. Res., C, 101, 3747–3764, 1996. 4922

Fetzner, S.: Bacterial dehalogenation, Appl. Microbiol. Biotechnol., 50, 633–657, 1998. 4921, 4926
Geen, C. E.: Selected marine sources and sinks of bromoform and other low molecular weight organobromines, Ph.D. thesis, Dalhousie, Univ. Halifax, Nova Scotia, 1992. 4921
Hense, I. and Beckmann, A.: Revisiting subsurface chlorophyll and phytoplankton distributions, Deep-Sea Res. Pt. I, 55, 1193–1199, doi:10.1016/j.dsr.2008.04.009, 2008. 4929, 4930, 4942
Burchard, H., Bolding, K., Kühn, W., Meister, A., Neumann, T., and Umlauf, L.: Description of a flexible and extendable physical biogeochemical model system for the water column, J. Mar. Syst., 61, 180–211, 2006.
Hughes, C., Malin, G., Nightingale, P. D., and Liss, P.: The effect of light stress on the release of volatile iodocarbons by three species of marine microalgae, Limnol. Oceanogr., 51, 2849–2854, 2006. 4924
Jakopitsch, C.: Catalase-peroxidase from *Synechocystis* is capable of chlorination and bromination reactions, Biochemical and biophysical research communications, 287–682, 2001. 4924
Karlsson, A., Auer, N., Schulz-Bull, D., and Abrahamsson, K.: Cyanobacterial blooms in the Baltic- A source of halocarbons, Mar. Chem., 110, 129–139, 2008. 4921, 4924
Lomas, M. W. and Lipschultz, F.: Forming the primary nitrite maximum: nitrifiers or phytoplankton?, Limnol. Oceanogr., 51, 2453–2467, 2006. 4922
Manley, S. L.: Phytogenesis of halomethanes: A product of selection or a metabolic accident?, Biogeochemistry, 60, 163–180, 2002. 4921
Martínez-Marrero, A., Rodríguez-Santana, A., Hernández-Guerra, A., Fraile-Nuez, E., López-Laatzen, F., Vélez-Belchí, P., and Parrilla, G.: Distribution of water masses and diapycnal mixing in the Cape Verde Frontal Zone, Geophys. Res. Lett., 35, L07609, doi:10.1029/2008GL033229, 2008. 4922
Moore, R. M. and Tokarczyk, R.: Volatile biogenic halocarbons in the northwest Atlantic, Global Biogeochem. Cy., 7, 195–210, 1993. 4921
Moore, R. M., Geen, C. E., and Tait, V. K.: Determination of Henrys law constants for a suite of naturally occuring halogenated methanes in seawater, Chemosphere, 30, 1183–1191, 1995. 4925
Moore, R. M., Webb, M., Tokarczyk, R., and Wever, R.: Bromoperoxidase and iodoperoxidase enzymes and production of halogenated methanes in marine diatom cultures, J. Geophys. Res., C, 101, 20 899–20 908, 1996. 4921, 4923, 4924, 4925, 4932

Nightingale, P. D., Malin, G., Law, C. S., Watson, A. J., Liss, P., Liddicoat, M. I., Boutin, J., and Upstill-Goddard, R. C.: In situ evaluation of air-sea gas exchange parameterizations using novel conservative and volatile tracers, Global Biogeochem. Cy., 14, 373–387, 2000. 4925

Olson, R.: Differential photoinhibition of marine nitrifying bacteria: A possible mechanism for the formation of the primary nitrite maximum, J. Mar. Res., 39, 227–238, 1981. 4922, 4926

Platt, U. and Hönninger, G.: The role of halogen species in the troposphere, Chemosphere, 52, 325–338, 2003. 4920

Prather, M. J., McElroy, M. B., and Wofsky, S. C.: Reductions in ozone at high concentrations of stratospheric halogens, Nature, 312, 227–231, 1984. 4920

Quack, B. and Wallace, D. W. R.: Air-sea flux of bromoform: Controls, rates, and implications, Global Biogeochem. Cy., 17, 1023, doi:10.1029/2002GB001890, 2003. 4921, 4925

Quack, B., Atlas, E., Petrick, G., Stroud, V., Schauffler, S., and Wallace, D. W. R.: Oceanic bromoform sources for the tropical atmosphere, Geophys. Res. Lett., 31, L23S05, doi:10.1029/2004GL020597, 2004. 4920, 4921, 4927, 4928, 4929, 4932, 4938, 4942

Quack, B., Peeken, I., Petrick, G., and Nachtigall, K.: Oceanic distribution and sources of bromoform and dibromomethane in the Mauritanian upwelling, J. Geophys. Res., C, 112, C10006, doi:10.1029/2006JC003803, 2007. 4921, 4932

Read, K. A., Mahajan, A. S., Carpenter, L. J., Evans, M. J., Faria, B. V. E., Heard, D. E., Hopkins, J. R., Lee, J. D., Moller, S. J., Lewis, A. C., Mendes, L., McQuaid, J. B., Oetjen, H., Saiz-Lopez, A., Pilling, M. J., and Plane, J. M. C.: Extensive halogen-mediated ozone destruction over the tropical Atlantic Ocean, Nature, 453, 1232–1235, 2008. 4920

Schall, C., Heumann, K. G., Mora, S. D., and Lee, P. A.: Biogenic brominated and iodinated organic compounds in ponds on the McMurdo Ice Shelf, Antarctica, Antarct. Sci., 8, 45–48, 1996. 4921

Schartau, M. and Oschlies, A.: Simultaneous data-based optimization of a 1D-ecosystem model at three locations in the North Atlantic Ocean: Part I: Method and parameter estimates, J. Mar. Res., 61, 765–793, 2003. 4923

Sinnhuber, B. M. and Folkins, I.: Estimating the contribution of bromoform to stratospheric bromine and its relation to dehydration in the tropical tropopause layer, Atmos. Chem. Phys., 6, 4755–4761, 2006, http://www.atmos-chem-phys.net/6/4755/2006/. 4920

Umlauf, L., Bolding, K., and Burchard, H.: GOTM Scientific Documentation. Version 3.2, in: Marine Science Reports, Baltic Sea Research Institute, Warnemünde, Germany, Vol. 63,

p. 231, 2005. 4922
Uppala, S., Kallberg, P., Simmons, A., Andrae, U., da Costa Bechtold, V., Fiorino, M., Gibson, J., Haseler, J., Hernandez, A., Kelly, G., Li, X., Onogi, K., Saarinen, S., Sokka, N., Allan, R., Andersson, E., Arpe, K., Balmaseda, M., Beljaars, A., van de Berg, L., Bidlot, J., Bormann, N., Caires, S., Chevallier, F., Dethof, A., Dragosavac, M., Fisher, M., Fuentes, M., Hagemann, S., Holm, E., Hoskins, B., Isaksen, L., Janssen, P., Jenne, R., McNally, A., Mahfouf, J.-F., Morcrette, J.-J., Rayner, N., Saunders, R., Simon, P., Sterl, A., Trenberth, K., Untch, A., Vasiljevic, D., Viterbo, P., and Woollen, J.: The ERA-40 re-analysis, Q. J. Roy. Meteor. Soc., 131, 2961–3012, 2005. 4927
Vogel, T. M., Criddle, C. S., and McCarthy, P. L.: Transformation of halogenated aliphatic compounds, Env. Sc. Technol., 21, 722–736, 1987. 4921
von Glasow, R., von Kuhlmann, R., Lawrence, M. G., Platt, U., and Crutzen, P. J.: Impact of reactive bromine chemistry in the troposphere, Atmos. Chem. Phys., 4, 2481–2497, 2004, http://www.atmos-chem-phys.net/4/2481/2004/. 4920
Wahman, D. G., Katz, L. E., and Speitel, J. G. E.: Cometabolism of Trihalomethanes by *Nitrosomonas europaea*, Appl. Environ. Microb., 71, 7980–7986, 2005. 4921, 4933
Wallace, D. W. R. and Bange, H. W.: Introduction to special section: Results of the Meteor 55: Tropical SOLAS Expedition, Geophys. Res. Lett., 31, L23S01, doi:10.1029/2004GL021014, 2004. 4922
Weber, L., Völker, C., Oschlies, A., and Burchard, H.: Iron profiles and speciation of the upper water column at the Bermuda Atlantic Time-series Study site: a model based sensitivity study, Biogeosciences, 4, 689–706, 2007, http://www.biogeosciences.net/4/689/2007/. 4922, 4923

Table 1. Overview of experiments and selected results: observed and simulated bromoform concentrations (nmol $CHBr_3$ m^{-3}) at the surface and in the subsurface maximum as well as air-sea flux (pmol $CHBr_3$ m^{-2} h^{-1}) for the month of November. Observed data are averages of offshore stations from the cruise M55 (Quack et al., 2004) west of 23° W.

	$CHBr_3$ source	$CHBr_3$ sink	surf. conc. nmol m^{-3}	max. conc. nmol m^{-3}	air-sea flux pmol m^{-2} h^{-1}
observations			5.0	24.8	175
EXP1	Q_1	S_1	6.5	21.5	163
EXP2	Q_1	S_2	6.5	20.9	169
EXP3	Q_1	S_3	6.7	23.6	188
EXP4	Q_2	S_3	6.7	23.6	188

BGD
5, 4919–4944, 2008

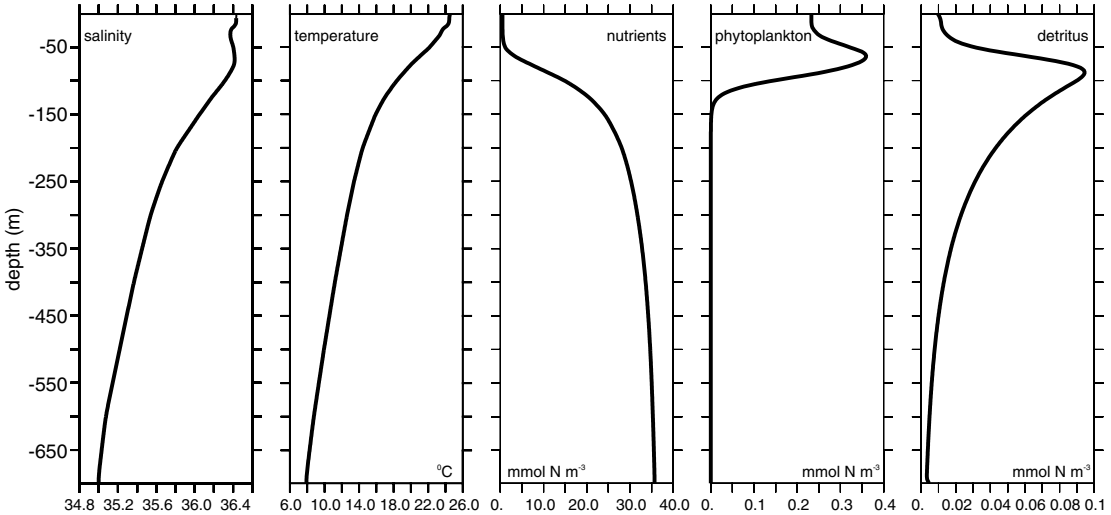

Fig. 1. Simulated annual mean vertical profiles of salinity, temperature, nutrients, phytoplankton and detritus.

BGD
5, 4919–4944, 2008

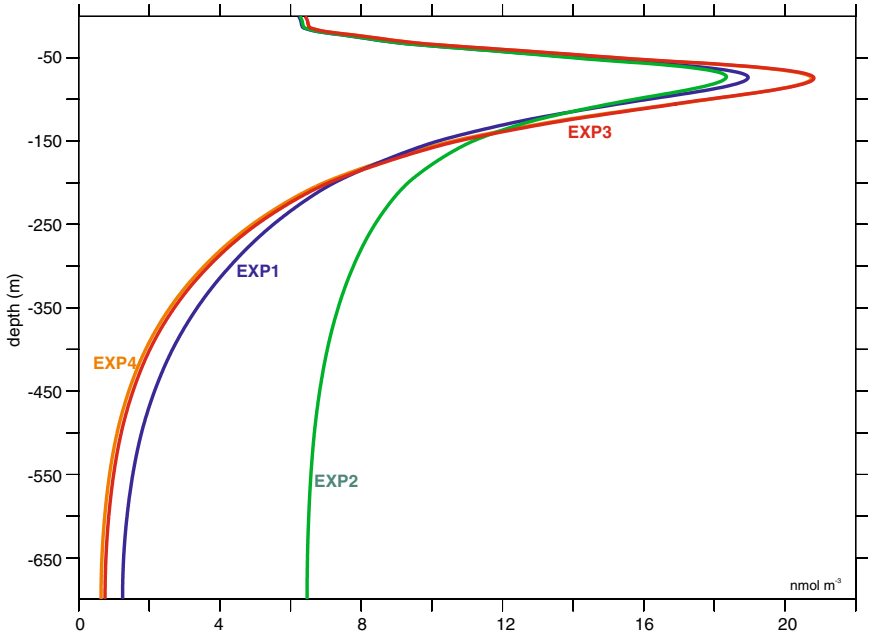

Fig. 2. Simulated annual mean vertical profiles of bromoform from the different experiments.

BGD

5, 4919–4944, 2008

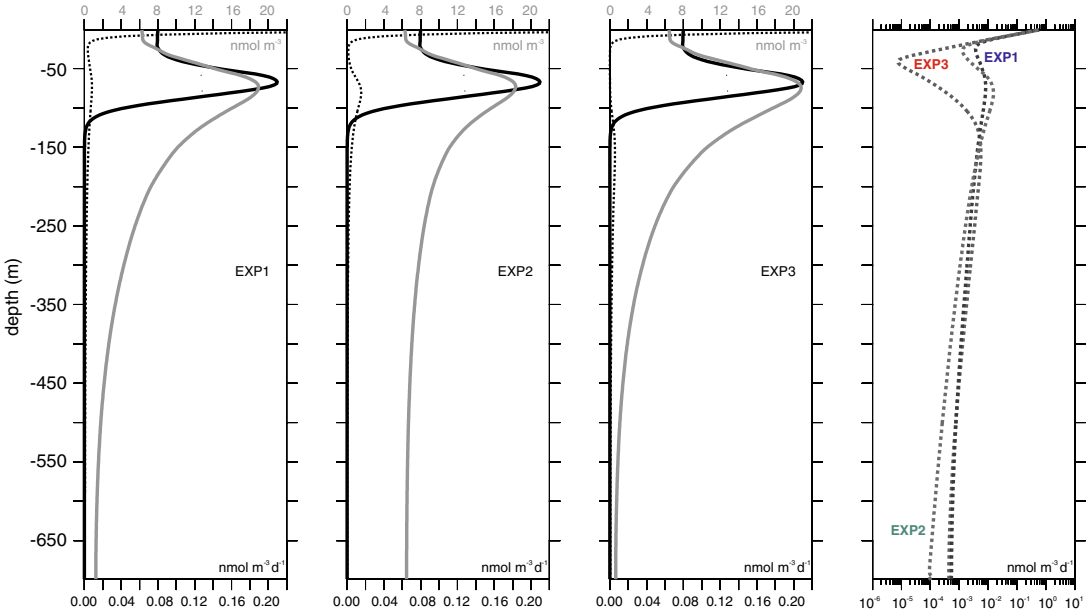

Fig. 3. Simulated annual mean vertical profiles of production (solid black line), loss (dotted black line) and bromoform (grey line, [nmol m^{-3}]) for the EXP1–EXP3 (EXP4 is similar to EXP3 an thus omitted). For a better visualization of the losses an additional plot with logarithmic scale is included (right).

BGD
5, 4919–4944, 2008

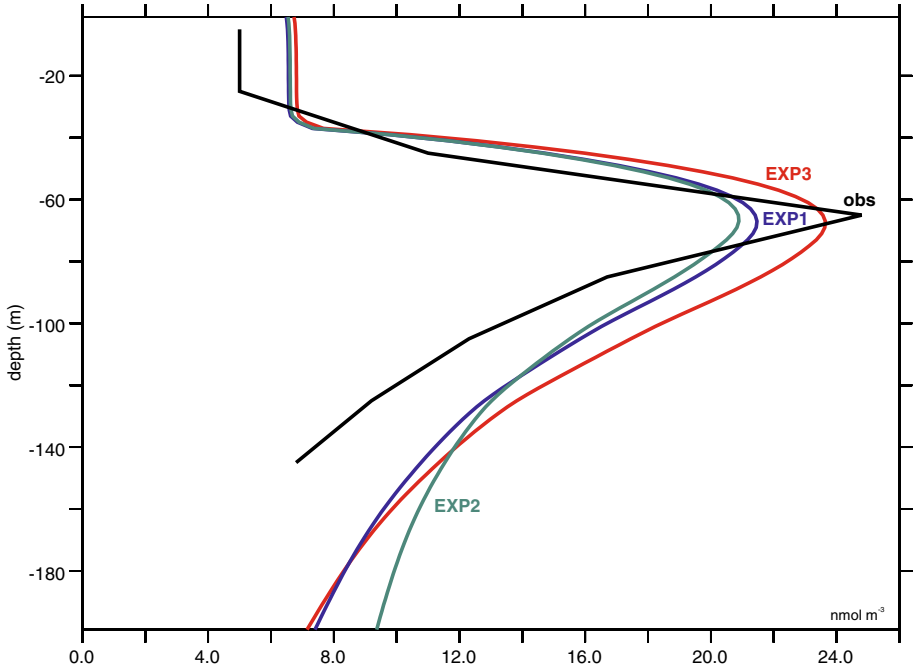

Fig. 4. Vertical profiles of observed (B_{obs}, black line) and simulated (EXP1: blue line, EXP2: green line, EXP3: red line) $CHBr_3$ concentrations from November. $CHBr_3$ profiles of stations which were closest to the Cape Verde station (area: 10.5–11.97° N, 16.83–25° W) from the cruise M55 in November 2002 (Quack et al., 2004) have been adjusted to the depth of the maximum of bromoform according to the method introduced by Hense and Beckmann (2008).

BGD
5, 4919–4944, 2008

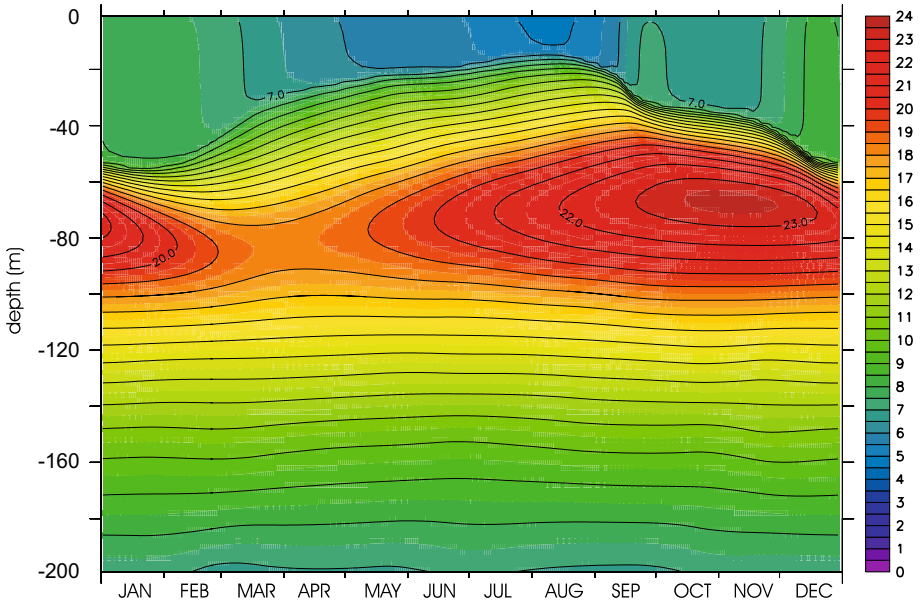

Fig. 5. Seasonal cycle of simulated bromoform concentrations in EXP3 in the upper 200 m. The contour interval is 1 nmol $CHBr_3$ m^{-3}.

BGD
5, 4919–4944, 2008

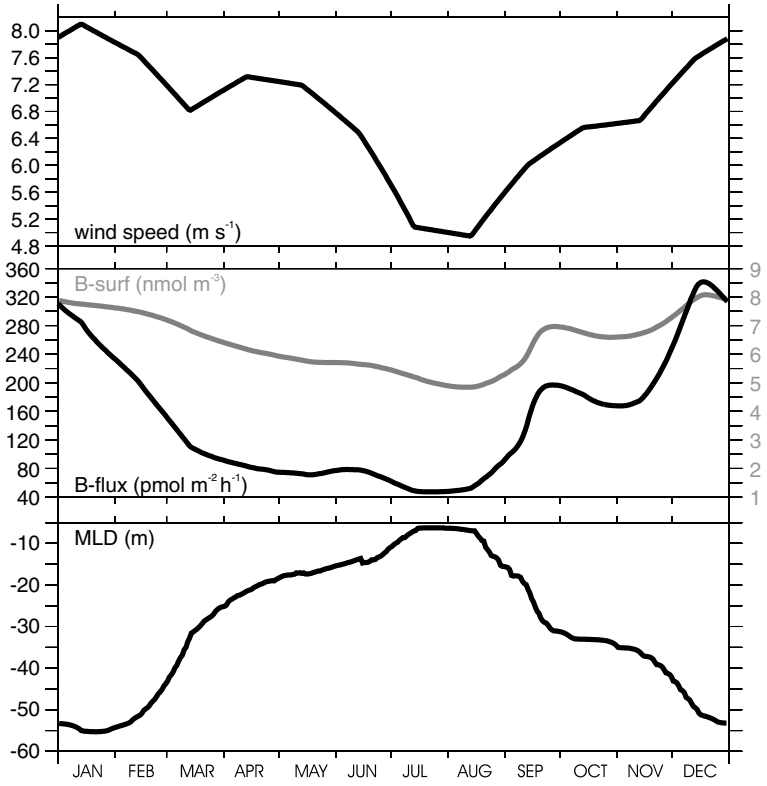

Fig. 6. Seasonal cycle of a) mixed layer depth (m), b) air-sea flux (solid black line, left axis) and surface concentrations (dotted grey line, right axis) of bromoform and c) wind speed in EXP3.

BGD
5, 4919–4944, 2008